Use of Spectral Analysis of Singular Values as a Test Metric for IMMAT Trials

Michael Hale, Jacob Davis, William Barber, James Akers

One of many challenges in the implementation of multiple exciter testing is establishing a reasonable set of test metrics to measure the quality of testing. This is especially true in the application of Impedance Matched Multi-Axis Testing; in that it is possible to have very large spectral density matrices that serve as reference criteria. While there exist plotting schemes to view a spectral density matrix, it is often necessary to break the overlay of reference and test results into subsections of the matrices to get sufficient resolution to interpret the data. In addition, as one attempts to control multiple locations on a structure, implementation of classical single degree-of freedom test tolerances across all channels and associated cross spectra is simply not feasible. Hence it is challenging to evaluate overall test quality. The use of spectral views of the dominant singular values from the singular value decomposition of the spectral density matrices and metrics based upon them is proposed for establishing a set of compact metrics for evaluating test quality. A laboratory experiment will be included to demonstrate this proposed technique.

INTRODUCTION

Multi-exciter testing (MET) continues to grow across the dynamic test community. The basic concepts of MET testing and fundamentals of multiple-degree-of-freedom (MDOF) signal processing are provided in Method 527 of MIL-STD-810 [1]. Detailed discussions of MDOF signal processing are addressed by Bendat and Piersol [2]. Establishing a reasonable set of test metrics to measure the quality of multiple-degree-of-freedom vibration testing continues to be a difficult challenge. A proposed approach to utilize a Singular Value Decomposition (SVD) of the Spectral Density Matrix (SDM) for this purpose is presented in this document.

Impedance Matched Multi-Axis Test (IMMAT), a special class of MET, will be discussed later in this document as an example of how this proposed approach can be applied. While most MET scenarios will have multiple references (at least one per degree of freedom), the IMMAT approach is characterized by a large number of references to address unique vibration environments at multiple locations throughout the structure of the test article. Consider a situation in which a *m x m x d* spectral density matrix (SDM), with *m* representing the number of control points and *d* the number of spectral lines or frequencies the SDM is computed at, is employed as a spectral based reference criteria for an MDOF test [3][4].

The IMMAT example in this document shows how this proposed approach can be applied. It had a 16 control point criteria, a 2 kHz bandwidth of interest, and a spectral resolution of 1.25 Hz. Therefore, each spectral based reference criteria $SDM_{ref}(f) \in C^{16x16}$ is a *16 x 16* complex matrix and there are 1601 of them spanning the entire frequency range $(f_1\ ,\ f_2\ , \ldots\ ,\ f_{1601})$.

PROPOSED APPROACH

The following discussion lays out the basic concepts to address the dilemma stated above. Consider the general matrix notation for a SDM as shown in Equation 1:

Equation 1: Spectral Density Matrix

$$[SDM_{xx}(f,T)] = \frac{2}{nT}\sum_{i=1}^{n_d} \begin{Bmatrix} X_1(f,t) \\ X_2(f,t) \\ \vdots \\ X_N(f,t) \end{Bmatrix}_i \{X_1^*\ X_2^*\ \ldots\ X_N^*\}_i$$

*Conducted under contract to the US Army Redstone Test Center

where, $X_N(f,t)$ is the discrete Fourier transform of the N^{th} time sequence $x_N(t)$ of each frame i of length T [5]. Each discrete Fourier transform is assumed to a be single sided DFT (real frequency) and to have been windowed as appropriate for random data.

In considering the most trivial of mechanical systems, it is well known that the eigenvalues of a system are correlated to the systems natural frequences. In the more complex case of a SDM, one could theorize that it would be desirable to have a high correlation to the dominant eigenvalues when comparing test results to associated reference criteria.

One technique to isolate the dominant characteristics of a matrix is the use of the Singular Value Decomposition. The use of computing the SVD on a SDM of test measured responses and plotting the singular values is a common frequency-domain modal identification technique used in Operational Modal Analysis (OMA) [6, 7, 8]. For a linear system, with *n* inputs and *m* outputs, the SDM of the measured output response $G_{YY}(f)$,which is an *m x m* complex matrix that is a function of the system frequency response function $H(f) \in C^{mxn}$, which is an *m x n* complex matrix, and the SDM of its input excitation $G_{XX}(f)$, which is an *n x n* complex matrix, and can be written as $G_{YY}(f) = H(f)G_{XX}(f)H^*(f)$ where * denotes the complex conjugate transpose.

As $G_{XX}(f)$ becomes closer to a scaled identity matrix, then $G_{YY}(f)$ becomes more dominated by the modes of the system and less dominated by the dynamics contained in the input excitation. This is exactly what drives the input excitation assumptions that OMA is based upon: the input excitation is broadband random, spatially distributed, uncorrelated, and stationary. If these assumptions hold and the spectral resolution used in computing $G_{YY}(f)$ is sufficiently fine enough to separate the modes of the system, then peaks in the largest singular value indicate structural modes of the system. These peak frequencies are good estimates of the modal frequencies, and the associated singular vectors are good estimates of the corresponding mode shapes. However, the user needs to exercise caution. If these assumptions are not met, principally if the input excitation contains sinusoidal components, these sinusoidal components will also produce peaks in the singular value plots that falsely indicate structural modes. However, peaks in the singular values due to a tone will generate a peak at the frequency of the tone in many if not all of the singular values.

Also, in Experimental Modal Analysis (EMA), the plot of the singular values from the SVD of the frequency response function $H(f)$ yields the Complex Mode Indicator (CMIF) function that is also used for identification of modal parameters [9,10]. For well separated modes, peaks in the CMIF correspond provide a quick indicator of the modes effectively excited during the modal test.

Consider the general case for a SVD of any $\mathbf{M} \in C^{mxn}$ complex *m x n* complex matrix with rank p, where $p \leq \min(m,n)$. The singular value decomposition of M can be given by $\mathbf{M} = \mathbf{USV}^*$, where $\mathbf{U} \in C^{mxp}$ is a complex *m x p* unitary matrix, $\mathbf{S} \in R^{pxp}$ is a real *p x p* diagonal matrix with the singular values on the diagonal, and $\mathbf{V} \in C^{nxp}$ is a *n x p* complex unitary matrix (i.e., $\mathbf{U}^*\mathbf{U} = I_p$, $\mathbf{V}^*\mathbf{V} = I_p$, where I_p is the *p x p* identity matrix). All of the singular values are real and positive. It is assumed the singular values are arranged in descending order of magnitude down the diagonal of each **S** matrix as shown in Equation 2.

Equation 2: Singular Values

$$S = \begin{bmatrix} \sigma_1 & \square & \square \\ \square & \ddots & \square \\ \square & \square & \sigma_p \end{bmatrix}, \qquad \sigma_1 \geq \cdots \geq \sigma_p > 0$$

If in addition $m = n$, and **M** is Hermitian (i.e., $\mathbf{M}^* = \mathbf{M}$), then its eigenvalues are real, and its singular values equal the absolute value of its nonzero eigenvalues. Finally, if in addition M is positive definite (i.e., $\mathbf{M} > 0$), then its eigenvalues equal its singular values. Note that the eigenvalues of $\mathbf{M}^*\mathbf{M}$ equal the square of the eigenvalues of **M** [11,12].

It is assumed that both the spectral based reference criteria SDM_{ref} and laboratory test result SDM_{lab} are positive definite, by definition Hermitian, and are of dimension *m x m* (square).

The SVD's of the $SDM_{ref}(f)$ and $SDM_{lab}(f)$ will be computed at each frequency *f*. Since the singular values of *S* are arranged in descending order of magnitude down the diagonal (i.e., $\sigma_1 \geq \sigma_2 \geq \ldots \geq \sigma_m > 0$), the magnitudes of the

plots of singular value Autospectral Spectral Densities (ASD's) will also decrease in magnitude with increasing singular value number. Hence the first few singular values will be the dominant singular values, yielding a much more compact structure by which to evaluate the effectiveness of a vibration test to excite the dominant structural modes of the payload of interest. Computing the RMS of each singular value ASD and comparing it to the sum of the RMS of all singular value ASD's provides a means of tracking its significance.

Another advantage to employing an SVD approach as opposed to strictly viewing SDM terms is that the singular values also contain the effects of cross spectral density (CSD) terms. This is valuable for very flexible structures with varying levels of coherence between control points where it is otherwise difficult to determine the quality of the test based strictly the CSD data of large reference SDM's.

METHODOLOGY

Ideally, the field data acquisition process and instrumentation locations would be carefully planned and key issues such as exciter and control instrumentation placement would be optimized. The following is a stepwise approach to the use of the spectral analysis of singular values as a test metric for a random vibration MET. Steps 1-8 below can easily be coded for efficient implementation.

Step 1: Establish a positive definite spectral based reference criteria $SDM_{ref}(f)$ of dimension *m x m,* where *m* is the number of control channels for frequencies $f_1,\ldots,f_d$. This reference is typically based on field data measurements. There are cases in which a high-fidelity model may be employed to establish $SDM_{ref}(f)$ in the absence of measured field data, however field data should be used if available since it will accurately capture the modal characteristics of the unit under test.

Step 2: Conduct the random vibration test and record acceleration time histories of all control locations as well of other channels of interest. The control channels should directly correlate to the locations from which the SDM_{ref} was based. Note that the number of control channels typically exceeds the number of drive points (over-determined feedback).

Step 3: Compute the laboratory test result *m x m* $SDM_{lab}(f)$ at the same frequency resolution as $SDM_{ref}(f)$ was based on (i.e., $f_1,\ldots,f_d$).

Step 4: Compute the singular value decompositions of the *m x m* $SDM_{ref}(f)$ and $SDM_{lab}(f)$ matrices at each of the frequencies $f_1,\ldots,f_d$ as shown in Equation 3. Ensure the singular values are arranged in descending order of magnitude on the diagonal each matrix $S_{ref}(\mathrm{f})$ and $S_{lab}(\mathrm{f})$.

Equation 3: Singular Value Decomposition of $SDM_{ref}(f)$ and $SDM_{lab}(f)$

$$SVD\left[SDM_{ref}(f)\right] = U_{ref}(f)S_{ref}(f)V_{ref}^{*}(f), f = f_1,\ldots,f_d$$

$$S_{ref}(f) = \begin{bmatrix} \sigma_{ref\,1}(f) & \square & \square \\ \square & \ddots & \square \\ \square & \square & \sigma_{ref\,m}(f) \end{bmatrix}, \qquad \sigma_{ref\,1}(f) \geq \cdots \geq \sigma_{ref\,m}(f) > 0$$

$$SVD[SDM_{lab}(f)] = U_{ref}(f)S_{lab}(f)V_{lab}^{*}(f), f = f_1,\ldots,f_d$$

$$S_{lab}(f) = \begin{bmatrix} \sigma_{lab\,1}(f) & \square & \square \\ \square & \ddots & \square \\ \square & \square & \sigma_{lab\,m}(f) \end{bmatrix}, \qquad \sigma_{lab\,1}(f) \geq \cdots \geq \sigma_{lab\,m}(f) > 0$$

Step 5: For each singular value from the reference criteria and the laboratory test results, compute the root mean square (RMS) value as shown in Equation 4.

Equation 4: RMS Values of the Reference Criteria and Laboratory Test Results Singular Values

$$\sigma_{ref\ i\ rms} = \sqrt{\frac{1}{d}\sum_{k=1}^{d} \sigma_{ref\ i}^2\,(f_k)}, \qquad \sigma_{lab\ i\ rms} = \sqrt{\frac{1}{d}\sum_{k=1}^{d} \sigma_{lab\ i}^2\,(f_k)} \quad , i = 1, \dots, m$$

Step 6: For each singular value of the **S** matrix across dimension *d*, starting with the dominant (first) singular value, compute the ratio of the RMS of the i^{th} laboratory test results singular value to the RMS of the i^{th} reference criteria singular value. As shown in Equation 5.

Equation 5: Ratio of the RMS of Laboratory Test Results and Reference Criteria i^{th} Singular Values

$$\frac{\sigma_{lab\ i\ rms}}{\sigma_{ref\ i\ rms}} \times 100\%\,, \qquad i = 1, \dots, m$$

Compute the sum of the RMS of each reference criteria singular value as shown in Equation 6.

Equation 6: Sum of the RMS of Each Spectral Based Reference Criteria Singular Value

$$Ref_{rms\ sum} = \sum_{k=1}^{d} \sigma_{ref\ k\ rms}\,,$$

Compute the ratio of the RMS of the i^{th} reference criteria singular value to that of the sum of the RMS of each reference criteria singular value as shown in Equation 7.

Equation 7: Ratio of the RMS of i^{th} Reference Criteria Singular Value to Sum of the RMS of Each Reference Criteria Singular Value

$$\frac{\sigma_{ref\ i\ rms}}{Ref_{rms\ sum}} \times 100\%\,, \qquad i = 1, \dots, m$$

Finally compute the ratio of the cumulative sum of the RMS of the first *j* spectral based reference criteria singular values to the sum of the RMS of each spectral based reference criteria singular value as shown in Equation 8.

Equation 8: Ratio of the Cumulative Sum of the RMS of the First Reference Criteria Singular Values to the Sum of the RMS of Each Reference Criteria Singular Value

$$\frac{\sum_{k=1}^{j} \sigma_{ref\ k\ rms}}{Ref_{rms\ sum}} \times 100\%$$

Step 7: Populate the following table with the results of Steps 5 and 6.

Table 1: Singular Value Comparison Table Format

Singular Value #	$\frac{\sigma_{lab\ i\ rms}}{\sigma_{ref\ i\ rms}}$ **(%)**	$\frac{\sigma_{ref\ i\ rms}}{Ref_{rms\ sum}}$ **(%)**	$\frac{\sum_{k=1}^{j}\sigma_{ref\ k\ rms}}{Ref_{rms\ sum}}$ **(%)**
1			
2			
3			
4			
5			
⋮			

Because the singular values are arranged in descending order of magnitude, the associated magnitudes of the singular value ASD's will also be arranged in descending order of magnitude. One could set criteria such as ensuring the ratio in column three of Table 1 be within some range, $\pm$ 20 % for example, for the singular values that make up some percentage, X=80% for example, of the reference $Ref_{rms\ sum}$. Another technique could be to establish the percentage of $Ref_{rms\ sum}$ that is associated with the dominant SV ASD's that have well defined peaks.

Step 8: To get a spectral view of the SVD data, plot the reference criteria and laboratory test result singular value ASD's, with specific tolerance bands relative to the reference criteria singular values, for the dominant reference criteria singular values that were identified in Step 7.

The ASD of the i^{th} reference criteria singular value: $[\sigma_{ref\ i}(f_1) \quad \cdots \quad \sigma_{ref\ i}(f_d)]$

The ASD of the i^{th} laboratory test results singular value: $[\sigma_{lab\ i}(f_1) \quad \cdots \quad \sigma_{lab\ i}(f_d)]$

The tolerance bands selected for the example are the default ASD tolerance bands for a random vibration test as defined in MIL-STD-810H.

It is also of interest to view the sum of the reference criteria singular values at each spectral line (i.e., frequency) $\sum_{i=1}^{m}\sigma_{ref\ i}(f_k)$ and similarly the sum of laboratory test results singular values $\sum_{i=1}^{m}\sigma_{lab\ i}(f_k)$ to get a global view of performance.

EXAMPLE: Test Objective

An MET random vibration test using IMMAT test techniques to replicate the vibration environment of measurements acquired at multiple internal locations on a large instrumentation pod to be transported on a fixed-wing jet aircraft will be used to demonstrate the proposed technique. The 1800-pound pod was approximately 167 inches long with a 30-inch diameter and contained structurally similar mass simulants for all significant equipment/components. The external fiberglass shell contains a carbon fiber structure that supports a large steel platform that supports various pieces of equipment. The steel structure is lightly damped, and the various structures result in a modally dense system within the frequency range of interest (100-2000 Hz).

As is often the case in developmental tests, particularly early on during development, actual flight data was not available. As an alternative, the test reference criteria SDM_{ref} employed was computed from acceleration time histories acquired on the instrumented pod while it was exposed to high intensity acoustics in a reverberant chamber at levels characteristic of non-buffet jet aircraft environments.

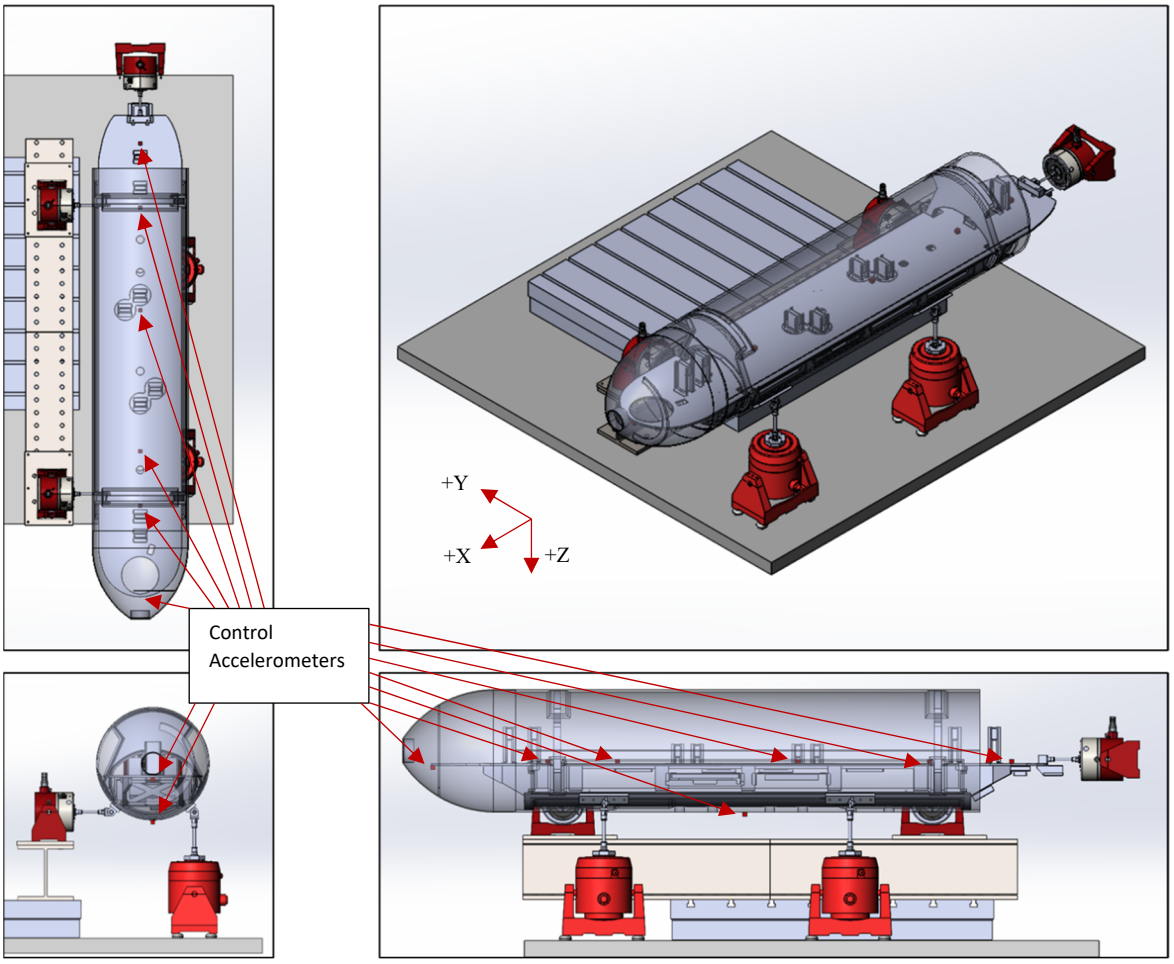

Figure 1: Display of Test Payload Configuration

EXAMPLE: Test Configuration

Five small to midsize electrodynamic shakers and 7 triaxial measurement locations were employed as illustrated in Figure 1. The weight of the 1800-pound pod was supported by an airbag isolation system (not shown in Figure 1 for clarity) that was adjusted to provide a suspension frequency below 5 Hz. Note that the pod arrived with preselected internal instrumentation locations based on the position of critical equipment within the pod. Post test reviews of the acoustic test results indicated several of the 21 measurement channels to be suspect. Therefore, only the 16 channels provided in Table 2 were selected for control in the laboratory IMMAT trials. All position information is with respect to a Cartesian reference frame with +X in the direction of flight and +Z towards the earth (i.e., downward). Orientation vectors are of the unit vector structure $[x, y, z]^T$ with origin $[0,0,0]^T$ defined as the forward most centerline location of the structure to which the accelerometers were placed. Observe that while all the instrumentation and drive lines of action in this example were either $[1,0,0]^T$, $[0,1,0]^T$ or $[0,0,1]^T$; in general, this is not a requirement.

Table 2: Control Instrumentation Placement

Control Ch	Orientation	Accelerometer Coordinates (inches)
1	(1,0,0)	(-7, 0, 0)
2	(0,1,0)	
3	(0,0,1)	
4	(1,0,0)	(-32, 0, 0)
5	(0,1,0)	
6	(0,0,1)	
7	(1,0,0)	(-98, 0, 0)
8	(0,1,0)	
9	(0,0,1)	
10	(0,1,0)	(-128, 0, 0)
11	(1,0,0)	(-145, 0, 0)
12	(0,1,0)	
13	(0,0,1)	
14	(1,0,0)	(-98, 0, -12)
15	(0,1,0)	
16	(0,0,1)	

Table 3 details the positions of each of the 5 shakers. Observe that the shaker placements were not placed relative the centerlines of the test payload. The weight of the pod was supported by a solid frame beneath, and airbags were placed between the frame and the pod to simulate a free-free boundary condition. The shakers were connected to the test payload at positions relative to the carbon fiber framework of the pod. The main carbon fiber substructure provided the only reasonably solid locations to which it was possible to attach the stingers. At the time of this publication, the finite element model of the instrumentation pod was incomplete, so initial placement of the shakers was based strictly on engineering judgement. Follow-on activities are planned to employ modeling and simulation techniques to optimize the number of shakers, size of the shakers, their placements, and their orientations.

Table 3: Drive Points

Drive (DAC #)	Attachment Coordinates (inches)	Drive Orientation	Shaker Random Force Rating (lbf-rms)
D1	(-129, 10.5, -8.25)	(0,1,0)	120
D2	(-39, 10.5, -8.25)	(0,1,0)	120
D3	(-157, 0, -8.25)	(1,0,0)	120
D4	(-109, 10.5, -8.25)	(0,0,1)	190
D5	(-49, 10.5, -8.25)	(0,0,1)	190

Referring to Figure 1, observe that all instrumentation locations (shown as small red squares on the model) to be employed as control channels for the IMMAT test were internal to the structure apart from the CG accelerometer. Ideally, one would prefer the control points to be at relatively solid points such as bulkheads near the anticipated drive points to have good coherence between the drive and control points. For the case at hand, there were several inches of separation between the drive and control points, which was not optimal. Had the opportunity to select instrumentation points been available earlier in the test sequence, alternative locations would have been proposed.

While using only 5 shakers to control 16 channels distributed across the structure, one would not expect to yield perfect replication. However, the IMMAT technique does minimize impedance mismatch between the field and laboratory environments, significantly improving the chance of success if the available shaker parameters (e.g. force, velocity, and displacement) are sufficient to address the environment of interest.

EXAMPLE: Post Test Analysis

As stated earlier, the reference criteria, SDM_{ref} for the subject case is dimension *16 x 16 x 1601*. The actual test bandwidth of interest was 100-2000 Hz. Clearly viewing a SDM of this size in not practical. Figure 2 illustrates the issue of plotting and evaluating a large SDM. To keep the image of reasonable size, only a *5 x 5 x 1601* subset of overlay plots specific to the Z axis, $[0,0,1]^T$, is provided in Figure 2. For plotting purposes, by taking advantage of the Hermitian structures, a normalized version of SDM_{ref} and SDM_{lab} was computed by means of dividing the magnitude of the upper triangular portion of CSD terms by $\sqrt{G_{xx_{mm}} G_{yy_{mm}}}$ to obtain coherences as shown in the upper triangular portion of Figure 2. The lower triangular portion has the associated phase information, which remains the same as the original unnormalized SDM's. The diagonal terms are the ASD terms of the original unnormalized SDM's. While a pattern of similarity exists, it is clearly difficult to associate a simple test metric for such a data set. Evaluating even the subset of the control channels presented in Figure 2 presents a challenge because of the amount of data present.

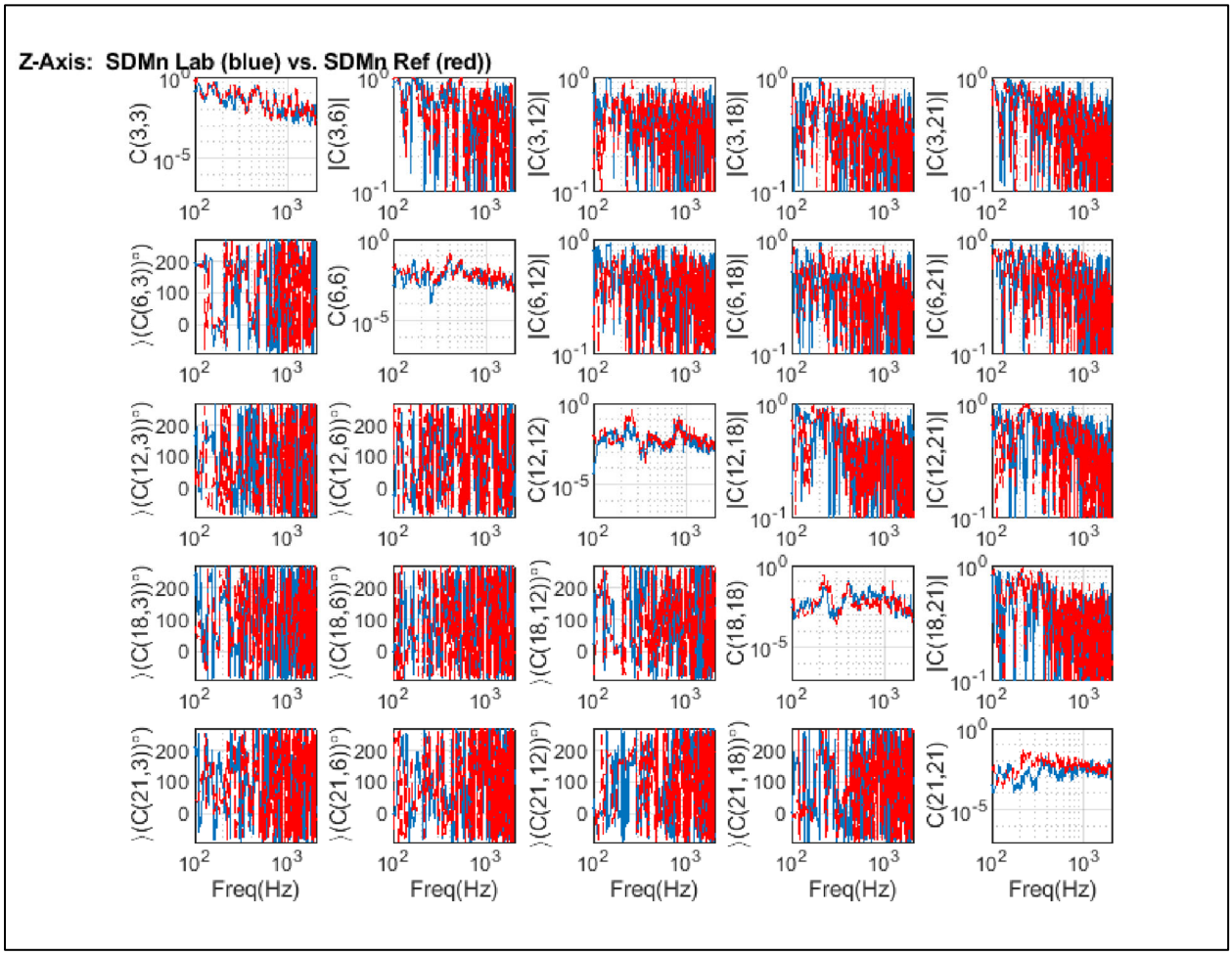

Figure 2: SDMref (red) vs. SDMlab (blue) for the Z-Axis Control Channels

Following Steps 4 and 5 above, ASD's of the singular values across depth *d* were computed. Figures 3a and 3b illustrate the ASD's of the 1st (*maximum*) singular value σ_1 and 2nd singular value σ_2, respectively, computed from the laboratory test results (green) overlaid with the corresponding spectral based reference criteria singular value ASD's (blue). The lower plots in Figures 3a and 3b show that the root mean square (RMS) of the 1st and 2nd singular value ASD's are 40% and 16%, respectively, of the sum of the RMS for all the spectral based reference criteria singular value ASD's. For spectral comparisons traditional ASD tolerances, ±3dB tolerance bands up to 500 Hz and ±6dB

between 500 and 2000 Hz, are also overlaid on Figures 3a and 3b. Observe that the engineering units on the ASD plots of Figures 3-6 are $\frac{G^2}{Hz}$. This led to the choice of placing traditional ASD tolerances on the singular value ASD plots of Figures 3a and 3b.

Figure 3a top plot compares the reference criteria 1st singular value ASD to the laboratory test results 1st singular value ASD. This clearly shows the initial test configuration is not sufficient to address major modal characteristics in the region between 200 Hz to 300 Hz. The valley in the laboratory test results 1st singular value around 260 Hz indicates the shakers were not located/orientated to adequately excite this mode(s). This is an example for which one would hope to have a finite element model of sufficient resolution to aid in making better and/or additional drive point selections to address the shortcoming. Assuming one made changes to the test such as variation of shaker locations/orientations or even the addition of additional shakers or control points, this same technique can be applied to the revised test configuration to determine if the changes yielded the desired improvements. This is certainly being planned for the example at hand.

Figure 3a bottom plot shows the ratio of the RMS of each of the 16 reference criteria singular values to sum of the RMS of each reference criteria singular values. This shows only about the first 6 reference criteria singular values are significant.

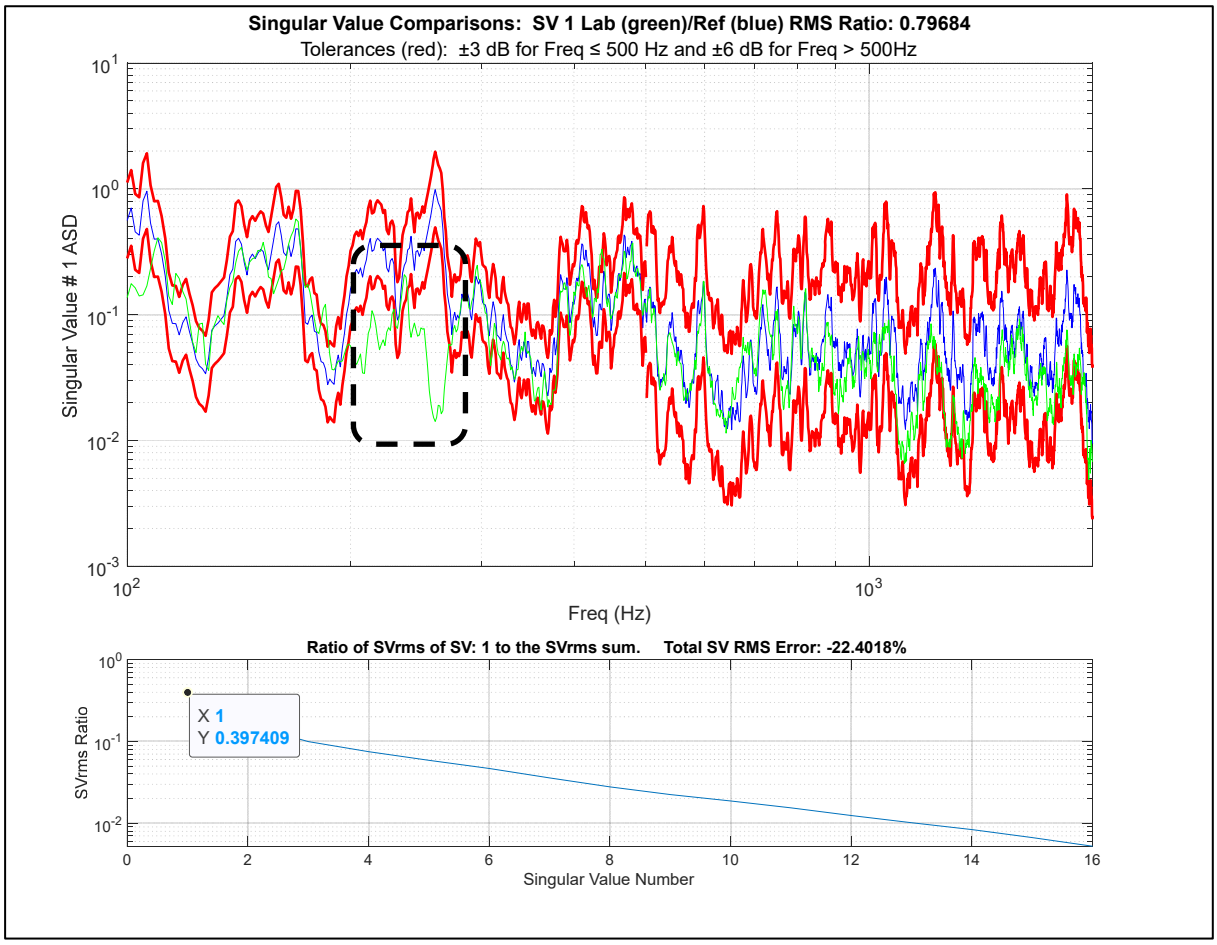

Figure 3a: Top Figure: 1st Singular Value ASD Comparison: Laboratory Test Results (green), Reference Criteria (blue), Upper & Lower Tolerance Bands (red), Frequency Range Not Well Excited During Lab Test (black dashed box).

Figure 3a: Bottom Figure: Ratio of the RMS of each of the 16 Reference Criteria Singular Values to Sum of the RMS of Each Reference Criteria Singular Value.

Figure 3b top plot compares the reference criteria 2nd singular value ASD to the laboratory test results 2nd singular value ASD. This also clearly shows the initial test configuration is not sufficient to address major modal characteristics in the region between 200 Hz to 300 Hz. Again, there is a valley in the laboratory test results 2nd singular value around 260 Hz.

Figure 3b bottom plot is the same and Figure 3a bottom plot, except the ratio with respect to the 2nd singular value called out.

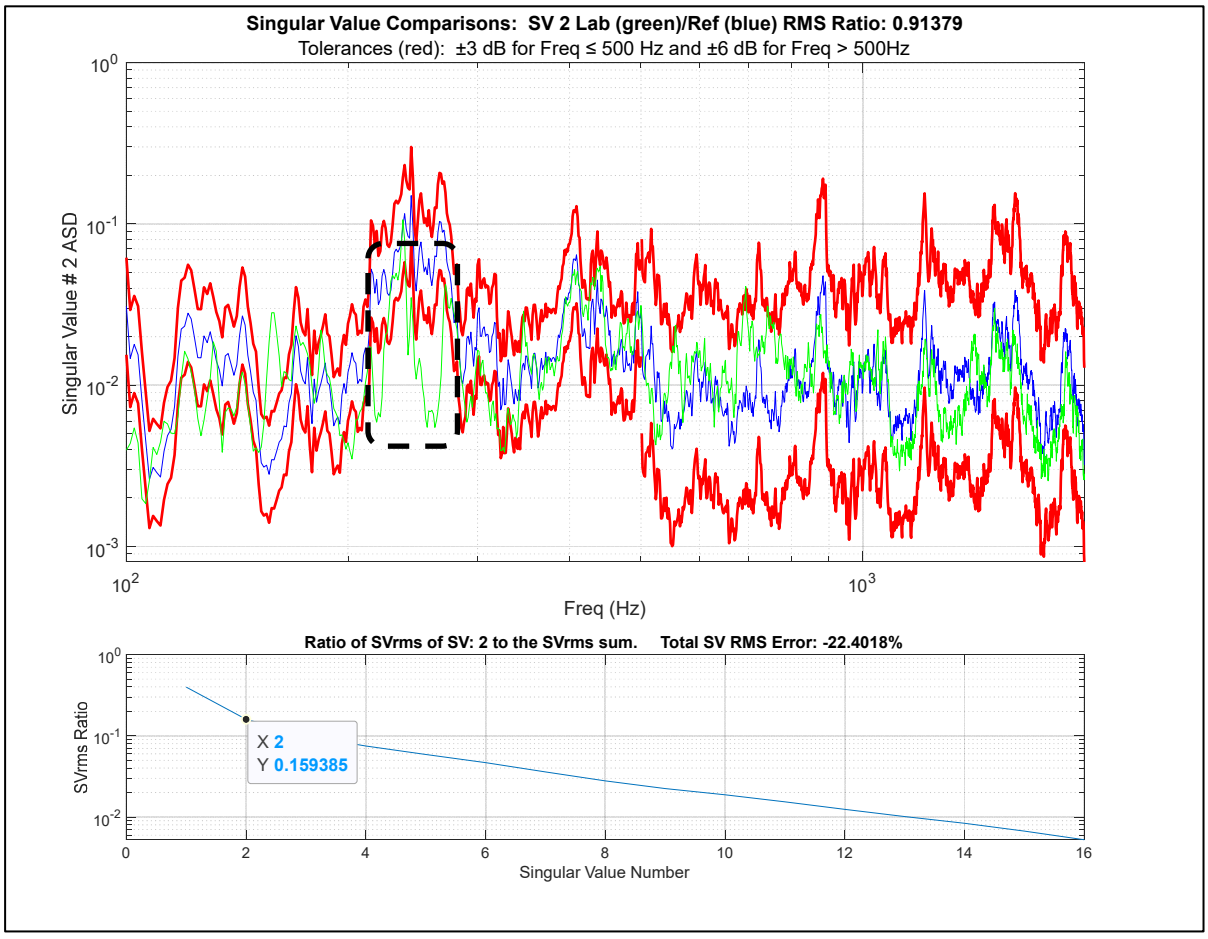

Figure 3b: Top Figure: 2nd Singular Value ASD Comparison: Laboratory Test Results (green), Reference Criteria (blue), Upper & Lower Tolerance Bands (red), Frequency Range Not Well Excited During Lab Test (black dashed box).

Figure 3b: Bottom Figure: Ratio of the RMS of each of the 16 Reference Criteria Singular Values to Sum of the RMS of Each Reference Criteria Singular Value.

Table 4 shows the ratios of the RMS ratios of the singular value ASD's for the first 6 singular values as defined in Steps 6 & 7 above. The 2nd column shows the laboratory test result RMS levels tend to be lower than the reference criteria. This is typical of an overdetermined feedback case for which a rectangular control scheme is required. Observe that the laboratory to reference RMS ratio is low for the sixth singular value ASD, however, it only represents 5% of the total of the sum of the SV RMS levels. The 4th column shows that for this example, 84% of the sum of the reference criteria singular value ASD RMS levels is contained in the first 6 singular values. Therefore, for this example, only the first 6 reference criteria singular values were considered potentially significant and participation percentages above the sixth singular value ASD's were considered negligible.

Table 4: Singular Value Comparison Table

Singular Value #	$\frac{\sigma_{lab\ i\ rms}}{\sigma_{ref\ i\ rms}}$ **(%)**	$\frac{\sigma_{ref\ i\ rms}}{Ref_{rms\ sum}}$ **(%)**	$\frac{\sum_{k=1}^{j}\sigma_{ref\ k\ rms}}{Ref_{rms\ sum}}$ **(%)**
1	80	40	40
2	91	16	56
3	96	10	66
4	90	7	73
5	81	6	79
6	65	5	84

Figures 4a and 4b compares the 1st and 2nd singular value ASD's of the reference criteria and laboratory test results to all 16 laboratory test results singular values and the sum at each frequency of the 16 reference criteria singular values. Note the modally dense nature of the test payload and indicated by the high density of peaks in the singular value ASD's. Clearly the first singular value of the reference criteria ASD addressed the majority of the envelop of the individual control channels in this case.

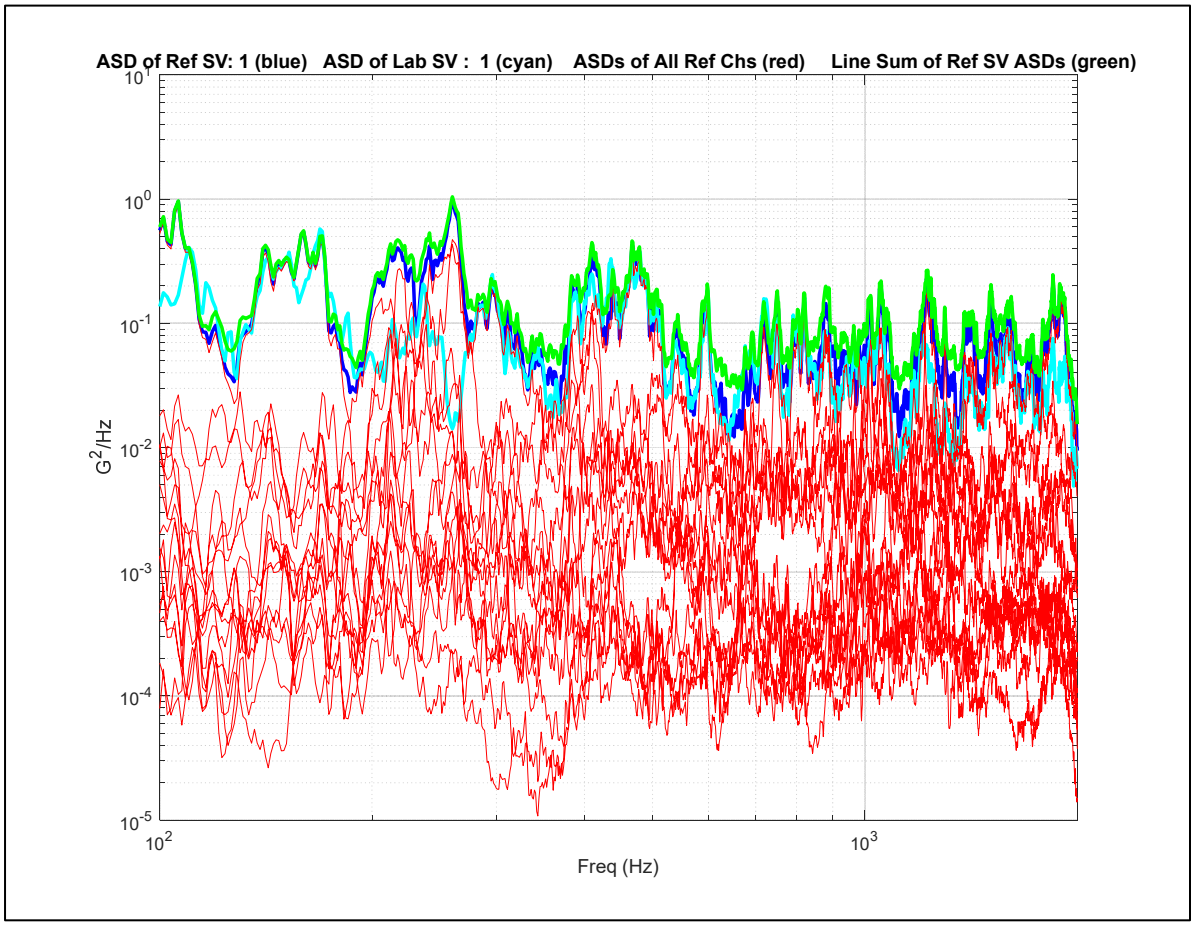

Figure 4a: Singular Value ASD Comparison: Reference Criteria 1st Singular Value (blue), Laboratory Test Results 1st Singular Value (cyan), All Laboratory Test Result Singular Values (red), Sum of the Reference Criteria Singular Values at Each Frequency (green).

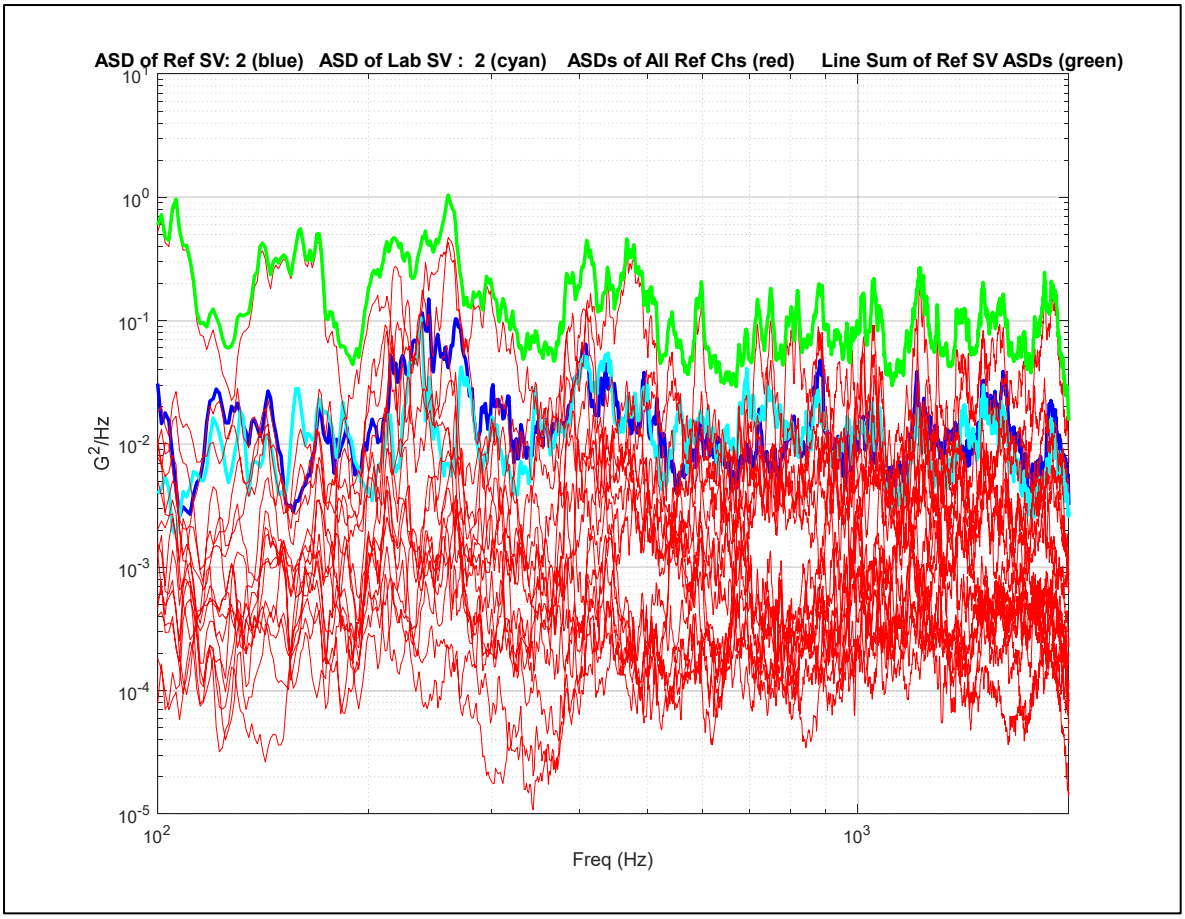

Figure 4b: Singular Value ASD Comparison: Reference Criteria 2nd Singular Value (blue), Laboratory Test Results 2nd Singular Value (cyan), All Laboratory Test Result Singular Values (red), Sum of the Reference Criteria Singular Values at Each Frequency (green).

Figure 5 shows the ASD's of the first 6 reference criteria singular values vs. the sum of the sixteen reference criteria singular values at each frequency. Note the descending amplitudes across the spectrum as the singular value number increases. Given the relationship between the singular values for this example and its natural frequencies, most of the energy associated with the modes is addressed by the first few reference criteria singular values ASD's.

The reference criteria 1st singular value ASD does not exhibit any valleys that would indicate modes of the test payload were not well excited during the acoustic test, except for modes in the two frequency bands corresponding to the two valleys between 100 Hz to 200 Hz. However, the reference criteria 2nd singular value ASD has peaks approximately located at these valleys, which indicates there are no modes in these regions. Hence the reference criteria ASDs therefore show the test payload was well excited during the acoustic test.

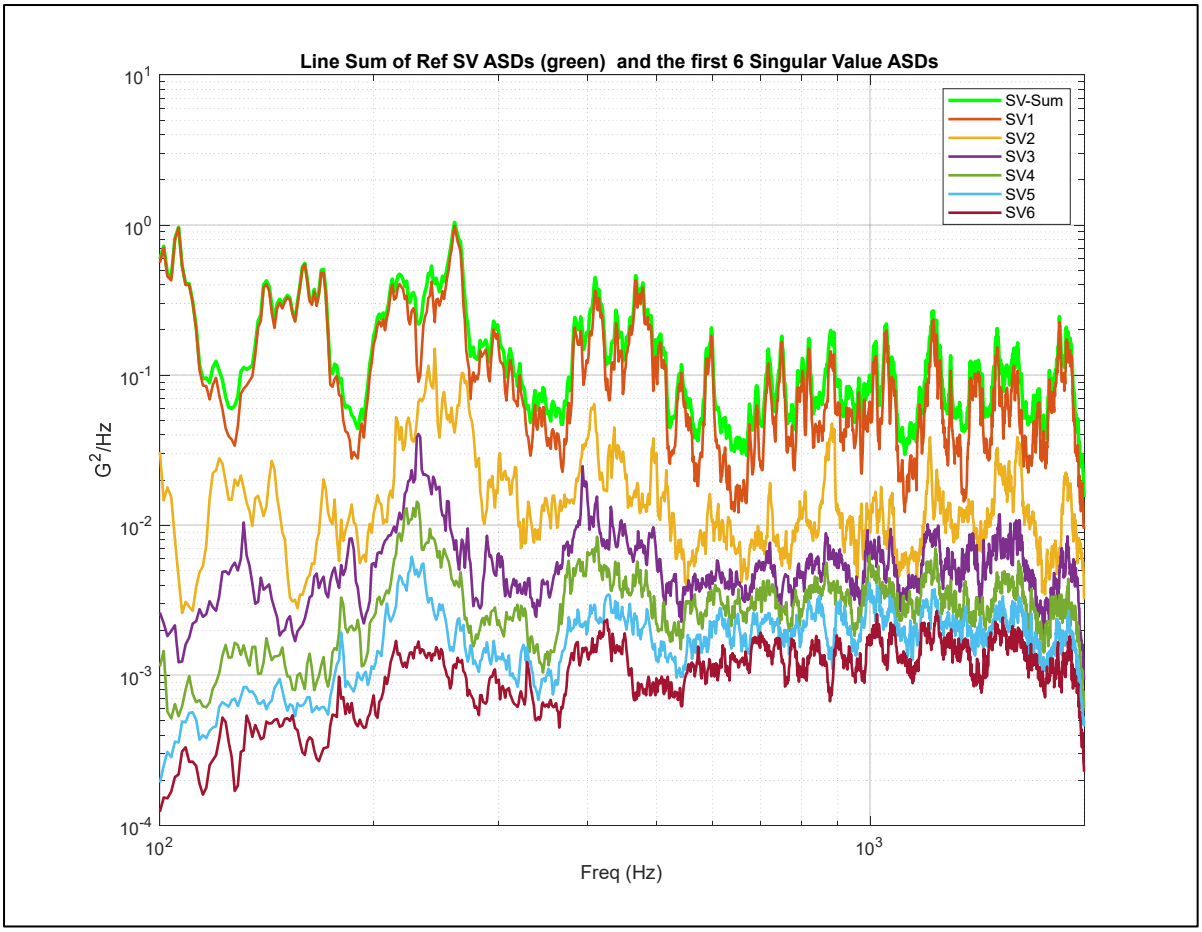

Figure 5: Reference Criteria Singular Value ASD Comparison: First 6 Singular Value ASD's and Sum of the Reference Criteria Singular Values at Each Frequency (green).

Figure 6 compares the sum of the reference criteria singular values at each frequency compared to the laboratory test results singular values along with the test tolerances. This comparison provides a global view of performance of the laboratory test in a single plot. As illustrated by the ASD of the first singular values, the mode in the 260 Hz region is clearly not being excited. As stated previously, the shaker placements for this original trial were based on judgement and positions on the test payload framework that were strong enough to connect a shaker and the instrumentation locations were preselected by a test customer. The next logical step would be to finish the finite element model and review modal analysis results to investigate alternate or additional drive points that would potentially yield better control. In addition, if given the opportunity, it would have been better to have been involved in the original instrumentation location selections, again verifying the need to be involved in test details as early in the test phase as possible.

Again, as suggested earlier, if changes are made to the test setup, use of the singular value ASD's and associated RMS levels serves as a compact metric to compare the modified test results to that of the previous runs. This technique will continue to be tested in future IMMAT test sequences as a metric to evaluate the objective of creating system level laboratory trials with high correlation to the measured field environment.

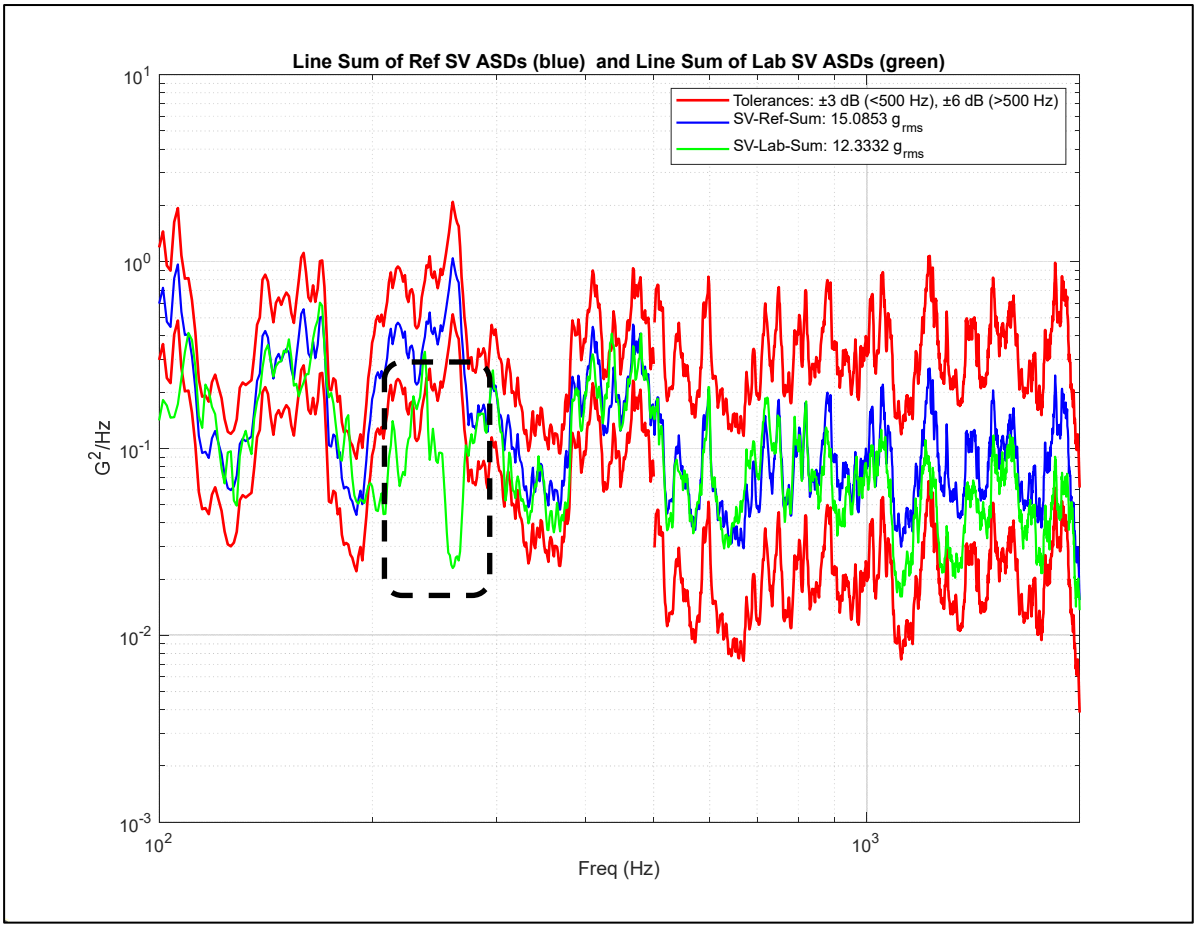

Figure 6: Line Sum Singular Value ASD Sums of Reference Criteria and Laboratory Test Results

CONCLUSIONS & FUTURE WORK

It has been shown that the use of the ASD's and RMS values of singular values computed from the SVD of the spectral based reference criteria $SDM_{ref}(f)$ and laboratory test results $SDM_{lab}(f)$ can serve as a compact test metric in the conduct of a MET random vibration test. Establishing acceptable singular value ASD spectral shape and RMS tolerances between reference criteria and laboratory test results should be studied further.

The discussion in this paper concentrated primarily on the singular values of the SVD of the spectral based reference criteria $SDM_{ref}(f)$ and laboratory test results $SDM_{lab}(f)$. Further research into the modal interpretation of the individual singular value ASD's and the associated singular vectors of the unitary matrix U, may provide more insight into the interpretation of deficiencies in the test levels and may help with optimization of complex multi-axis test setups such as IMMAT.

Additional mode shape data is associated with the singular vectors of the unitary matrix $\boldsymbol{U}$. For the example provided, the number and placement of accelerometers were not sufficient to extract meaningful mode shape information, especially for the higher frequencies.

It was observed in the example provided and other test examples that the quality of the match between reference and laboratory SVD ASD's was highest for first singular value through the singular value equal to the number of drive points. This observation will be studied further in future work.

Future work also includes tear down of the test payload, increasing the measurement channel count, and optimizing placement of the instrumentation based on finite element model-based predictions. The same is true for selection of

the number of shakers and optimal drive point locations within the limitations of the unique structural considerations of the instrumentation pod.

REFERENCES

[1] MIL-STD-810H: Department of Defense Test Method Standard, Environmental Engineering Considerations and Laboratory Tests, 31 January 2019.

[2] Bendat, Julius S. and Piersol, Allen G., *Random Data Analysis and Measurement Procedures*, 3rd ed., John Wiley & Sons, Inc., New York, 2000.

[3] P. R. Daborn and D. J. Ewins. "Replicating Aerodynamic Excitation in the Laboratory." *Proceedings of the 31st International Modal Analysis Conference*, Ca, 2013.

[4] C. Roberts and D. J. Ewins. "Multi-Axis Vibration Testing of an Aerodynamically Excited Structure." *Journal of Vibration and Control*, April 2016. doi: 10.1177/1077546316642064.

[5] Harris, C., Piersol, A. *Harris' Shock and Vibration Handbook* 5th ed., McGraw-Hill Handbooks, Ch 27, 2002.

[6] C.E. Ventura, R. Brincker, P. Anderson, "Dynamic Properties of the Painter Street Overpass at Different Levels of Vibration." *Proceedings of the 2005 Eurodyn Conference,* 2005.

[7] Ventura, Carlos and Brinker, Rune. *Introduction to Operational Modal Analysis*, Wiley, 2015.

[8] J. Akers, et al, "Operational Modal Analysis of the Artemis I Dynamic Rollout Test and Wet Dress Rehearsal", *Proceedings of the 42nd International Modal Analysis Conference*, 2024.

[9] Avitabile, Peter. *Modal Testing: A Practitioner's Guide*, Wiley, 2018.

[10] Allemang, Randall and Avitabile, Peter. *Handbook of Experimental Structural Dynamics*, Springer, 2022.

[11] Nobel, Ben and Daniel, James W. *Applied Linear Algebra* 3rd ed., United States of America, Prentice-Hall,1998.

[12] Horn, Roger and Johnson, Charles. *Matrix Analysis*, United States of America, Cambridge, 1991.

ABOUT THE AUTHORS

Michael Hale earned a Bachelor of Science in Electrical Engineering from Auburn University in 1983 and his Master of Science in Engineering and Doctor of Philosophy degrees from The University of Alabama in Huntsville (UAH) through the Electrical and Computer Engineering Department in 1992 and 1998, respectively. Dr. Hale has been employed as a principal research engineer with Trideum Corporation since 2015. Prior to retirement from 32 years of federal service, he was employed as senior electronics engineer and experimental developer in the Environmental and Component Test Directorate of the United States (US) Army Redstone Test Center (RTC), US Army Test and Evaluation Command (ATEC). Dr. Hale is an IEST Fellow and SAVE Lifetime Achievement Award recipient.

Contact: Michael T. Hale, PhD, mhale@trideum.com

Jacob Davis earned his Bachelor of Science and Master of Science in Mechanical Engineering degrees from The University of Alabama in 2017 and 2018, respectively. He is currently enrolled at the University of Alabama online working on his PhD coursework. Mr. Davis is currently employed as a Mechanical Engineer in the Environmental and Component Test Directorate of the US Army RTC, US ATEC, where he has worked since 2018.

Contact: Jacob A. Davis, jacob.a.davis91.civ@army.mil

William Barber is currently employed as the Senior Mechanical Engineer and Senior Experimental Developer in the Environmental and Component Test Directorate of the US Army RTC, US ATEC, where he has worked for more than 30 years. He earned a Bachelor of Science degree in Mechanical Engineering from Auburn University in 1992 and a Master of Science in Mechanical Engineering from UAH in 2005.

Contact: William (Bill) Barber, william.a.barber5.civ@army.mil

James Akers earned his Bachelor of Science, Master of Science, and Doctor of Philosophy in Aerospace Engineering degrees from the University of Michigan in 1983, 1985, and 1997, respectively. Dr. Akers is currently employed as a Senior Aerospace Engineer in the structural dynamics branch at NASA Glenn Research Center where he has been serving for the past 14 years. Prior to this he supported coupled loads analysis of United Launch Alliance launches from 2005 – 2010, was an engineering support contractor to GRC from 2000 - 2005, worked for ATA engineering from 1997 – 2000, and worked at the NASA Johnson Space Center from 1985 - 1990. Dr. Akers is an AIAA Associate Fellow and an SEM DeMichele award recipient.

Contact: James (Jim) Akers, james.c.akers-1@nasa.gov